

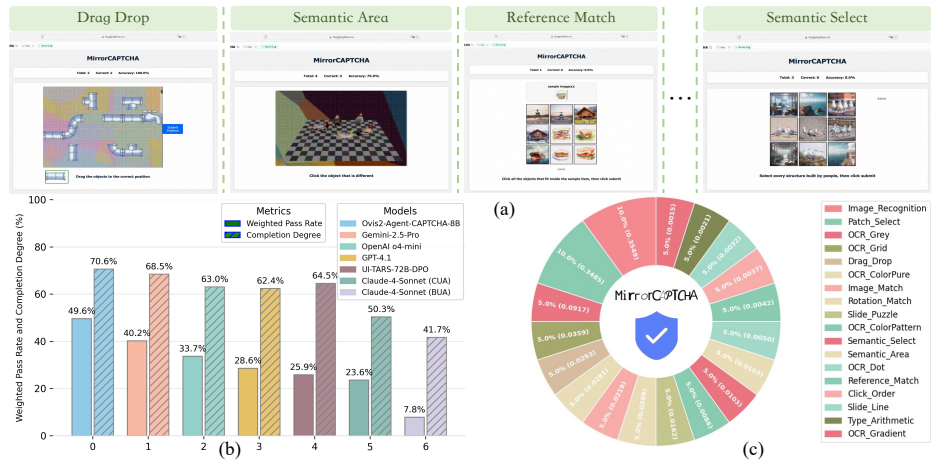
000 001 002 003 004 005 006 007 008 009 010 011 012 013 014 015 016 017 018 019 020 021 022 023 024 025 026 027 028 029 030 031 032 033 034 035 036 037 038 039 040 041 042 043 044 045 046 MIRRORCAPTCHA: WILD CAPTCHA, WILD DISTRIBUTION, WILD WEB-BASED PLATFORM MEET MULTIMODAL LLM AGENTS

006
007
Anonymous authors
008
Paper under double-blind review

ABSTRACT

013
014
015
016
017
018
019
020
021
022
023
024
025
026
027
028
029
030
031
032
033
034
035
036
037
038
039
040
041
042
043
044
045
046
The path to fully autonomous web agents is currently hindered by a critical bottleneck: their limited ability to handle CAPTCHA. Existing agent benchmarks largely ignore this practical challenge, failing to assess an agent's true capacity in cracking CAPTCHA. To bridge this gap, we comprehensively analyze the CAPTCHA distributions in the real world, and introduce **MirrorCAPTCHA** benchmark, annotated with *Weighted Pass Rate* and a novel proposed metric: *Completion Degree*. This benchmark is designed to serve as a “mirror” that accurately reflects the automation capabilities of agents in real scenarios. We filter out 2,095 websites from the Common Crawl, identifying the active CAPTCHA puzzles and classifying them into 18 distinct categories using the K-means clustering algorithm. To ensure practicality, we extract a web subgraph from Common Crawl covering these websites and employ random walks to simulate real-world CAPTCHA encounter frequencies, yielding a realistic measure of agents' ability. Additionally, we develop a lightweight synthetic data pipeline to train a model, Ovis2-Agent-CAPTCHA-8B, which significantly outperforms current state-of-the-art closed-source models on the MirrorCAPTCHA benchmark, achieving a 9.4% higher average *Weighted Pass Rate* and a 2.13% higher average *Completion Degree* compared with the second-place, Gemini-2.5-Pro.

1 INTRODUCTION



047
048
Figure 1: (a) Web-based CAPTCHA platform for evaluating web agents. (b) Performance of web agents. (c)
049
050
051
052
053
054
055
056
057
058
059
060
061
062
063
064
065
066
067
068
069
070
071
072
073
074
075
076
077
078
079
080
081
082
083
084
085
086
087
088
089
090
091
092
093
094
095
096
097
098
099
100
0101
0102
0103
0104
0105
0106
0107
0108
0109
0110
0111
0112
0113
0114
0115
0116
0117
0118
0119
0120
0121
0122
0123
0124
0125
0126
0127
0128
0129
0130
0131
0132
0133
0134
0135
0136
0137
0138
0139
0140
0141
0142
0143
0144
0145
0146
0147
0148
0149
0150
0151
0152
0153
0154
0155
0156
0157
0158
0159
0160
0161
0162
0163
0164
0165
0166
0167
0168
0169
0170
0171
0172
0173
0174
0175
0176
0177
0178
0179
0180
0181
0182
0183
0184
0185
0186
0187
0188
0189
0190
0191
0192
0193
0194
0195
0196
0197
0198
0199
0200
0201
0202
0203
0204
0205
0206
0207
0208
0209
0210
0211
0212
0213
0214
0215
0216
0217
0218
0219
0220
0221
0222
0223
0224
0225
0226
0227
0228
0229
0230
0231
0232
0233
0234
0235
0236
0237
0238
0239
0240
0241
0242
0243
0244
0245
0246
0247
0248
0249
0250
0251
0252
0253
0254
0255
0256
0257
0258
0259
0260
0261
0262
0263
0264
0265
0266
0267
0268
0269
0270
0271
0272
0273
0274
0275
0276
0277
0278
0279
0280
0281
0282
0283
0284
0285
0286
0287
0288
0289
0290
0291
0292
0293
0294
0295
0296
0297
0298
0299
0300
0301
0302
0303
0304
0305
0306
0307
0308
0309
0310
0311
0312
0313
0314
0315
0316
0317
0318
0319
0320
0321
0322
0323
0324
0325
0326
0327
0328
0329
0330
0331
0332
0333
0334
0335
0336
0337
0338
0339
0340
0341
0342
0343
0344
0345
0346
0347
0348
0349
0350
0351
0352
0353
0354
0355
0356
0357
0358
0359
0360
0361
0362
0363
0364
0365
0366
0367
0368
0369
0370
0371
0372
0373
0374
0375
0376
0377
0378
0379
0380
0381
0382
0383
0384
0385
0386
0387
0388
0389
0390
0391
0392
0393
0394
0395
0396
0397
0398
0399
0400
0401
0402
0403
0404
0405
0406
0407
0408
0409
0410
0411
0412
0413
0414
0415
0416
0417
0418
0419
0420
0421
0422
0423
0424
0425
0426
0427
0428
0429
0430
0431
0432
0433
0434
0435
0436
0437
0438
0439
0440
0441
0442
0443
0444
0445
0446
0447
0448
0449
0450
0451
0452
0453
0454
0455
0456
0457
0458
0459
0460
0461
0462
0463
0464
0465
0466
0467
0468
0469
0470
0471
0472
0473
0474
0475
0476
0477
0478
0479
0480
0481
0482
0483
0484
0485
0486
0487
0488
0489
0490
0491
0492
0493
0494
0495
0496
0497
0498
0499
0500
0501
0502
0503
0504
0505
0506
0507
0508
0509
0510
0511
0512
0513
0514
0515
0516
0517
0518
0519
0520
0521
0522
0523
0524
0525
0526
0527
0528
0529
0530
0531
0532
0533
0534
0535
0536
0537
0538
0539
0540
0541
0542
0543
0544
0545
0546
0547
0548
0549
0550
0551
0552
0553
0554
0555
0556
0557
0558
0559
0560
0561
0562
0563
0564
0565
0566
0567
0568
0569
0570
0571
0572
0573
0574
0575
0576
0577
0578
0579
0580
0581
0582
0583
0584
0585
0586
0587
0588
0589
0590
0591
0592
0593
0594
0595
0596
0597
0598
0599
0600
0601
0602
0603
0604
0605
0606
0607
0608
0609
0610
0611
0612
0613
0614
0615
0616
0617
0618
0619
0620
0621
0622
0623
0624
0625
0626
0627
0628
0629
0630
0631
0632
0633
0634
0635
0636
0637
0638
0639
0640
0641
0642
0643
0644
0645
0646
0647
0648
0649
0650
0651
0652
0653
0654
0655
0656
0657
0658
0659
0660
0661
0662
0663
0664
0665
0666
0667
0668
0669
0660
0661
0662
0663
0664
0665
0666
0667
0668
0669
0670
0671
0672
0673
0674
0675
0676
0677
0678
0679
0680
0681
0682
0683
0684
0685
0686
0687
0688
0689
0690
0691
0692
0693
0694
0695
0696
0697
0698
0699
0700
0701
0702
0703
0704
0705
0706
0707
0708
0709
0710
0711
0712
0713
0714
0715
0716
0717
0718
0719
0720
0721
0722
0723
0724
0725
0726
0727
0728
0729
0730
0731
0732
0733
0734
0735
0736
0737
0738
0739
0730
0731
0732
0733
0734
0735
0736
0737
0738
0739
0740
0741
0742
0743
0744
0745
0746
0747
0748
0749
0740
0741
0742
0743
0744
0745
0746
0747
0748
0749
0750
0751
0752
0753
0754
0755
0756
0757
0758
0759
0750
0751
0752
0753
0754
0755
0756
0757
0758
0759
0760
0761
0762
0763
0764
0765
0766
0767
0768
0769
0760
0761
0762
0763
0764
0765
0766
0767
0768
0769
0770
0771
0772
0773
0774
0775
0776
0777
0778
0779
0770
0771
0772
0773
0774
0775
0776
0777
0778
0779
0780
0781
0782
0783
0784
0785
0786
0787
0788
0789
0780
0781
0782
0783
0784
0785
0786
0787
0788
0789
0790
0791
0792
0793
0794
0795
0796
0797
0798
0799
0790
0791
0792
0793
0794
0795
0796
0797
0798
0799
0800
0801
0802
0803
0804
0805
0806
0807
0808
0809
0800
0801
0802
0803
0804
0805
0806
0807
0808
0809
0810
0811
0812
0813
0814
0815
0816
0817
0818
0819
0810
0811
0812
0813
0814
0815
0816
0817
0818
0819
0820
0821
0822
0823
0824
0825
0826
0827
0828
0829
0820
0821
0822
0823
0824
0825
0826
0827
0828
0829
0830
0831
0832
0833
0834
0835
0836
0837
0838
0839
0830
0831
0832
0833
0834
0835
0836
0837
0838
0839
0840
0841
0842
0843
0844
0845
0846
0847
0848
0849
0840
0841
0842
0843
0844
0845
0846
0847
0848
0849
0850
0851
0852
0853
0854
0855
0856
0857
0858
0859
0850
0851
0852
0853
0854
0855
0856
0857
0858
0859
0860
0861
0862
0863
0864
0865
0866
0867
0868
0869
0860
0861
0862
0863
0864
0865
0866
0867
0868
0869
0870
0871
0872
0873
0874
0875
0876
0877
0878
0879
0870
0871
0872
0873
0874
0875
0876
0877
0878
0879
0880
0881
0882
0883
0884
0885
0886
0887
0888
0889
0880
0881
0882
0883
0884
0885
0886
0887
0888
0889
0890
0891
0892
0893
0894
0895
0896
0897
0898
0899
0890
0891
0892
0893
0894
0895
0896
0897
0898
0899
0900
0901
0902
0903
0904
0905
0906
0907
0908
0909
0900
0901
0902
0903
0904
0905
0906
0907
0908
0909
0910
0911
0912
0913
0914
0915
0916
0917
0918
0919
0910
0911
0912
0913
0914
0915
0916
0917
0918
0919
0920
0921
0922
0923
0924
0925
0926
0927
0928
0929
0920
0921
0922
0923
0924
0925
0926
0927
0928
0929
0930
0931
0932
0933
0934
0935
0936
0937
0938
0939
0930
0931
0932
0933
0934
0935
0936
0937
0938
0939
0940
0941
0942
0943
0944
0945
0946
0947
0948
0949
0940
0941
0942
0943
0944
0945
0946
0947
0948
0949
0950
0951
0952
0953
0954
0955
0956
0957
0958
0959
0950
0951
0952
0953
0954
0955
0956
0957
0958
0959
0960
0961
0962
0963
0964
0965
0966
0967
0968
0969
0960
0961
0962
0963
0964
0965
0966
0967
0968
0969
0970
0971
0972
0973
0974
0975
0976
0977
0978
0979
0970
0971
0972
0973
0974
0975
0976
0977
0978
0979
0980
0981
0982
0983
0984
0985
0986
0987
0988
0989
0980
0981
0982
0983
0984
0985
0986
0987
0988
0989
0990
0991
0992
0993
0994
0995
0996
0997
0998
0999
0990
0991
0992
0993
0994
0995
0996
0997
0998
0999
1000
1001
1002
1003
1004
1005
1006
1007
1008
1009
1000
1001
1002
1003
1004
1005
1006
1007
1008
1009
1010
1011
1012
1013
1014
1015
1016
1017
1018
1019
1010
1011
1012
1013
1014
1015
1016
1017
1018
1019
1020
1021
1022
1023
1024
1025
1026
1027
1028
1029
1020
1021
1022
1023
1024
1025
1026
1027
1028
1029
1030
1031
1032
1033
1034
1035
1036
1037
1038
1039
10310
10311
10312
10313
10314
10315
10316
10317
10318
10319
10320
10321
10322
10323
10324
10325
10326
10327
10328
10329
10330
10331
10332
10333
10334
10335
10336
10337
10338
10339
103310
103311
103312
103313
103314
103315
103316
103317
103318
103319
103320
103321
103322
103323
103324
103325
103326
103327
103328
103329
103330
103331
103332
103333
103334
103335
103336
103337
103338
103339
1033310
1033311
1033312
1033313
1033314
1033315
1033316
1033317
1033318
1033319
1033320
1033321
1033322
1033323
1033324
1033325
1033326
1033327
1033328
1033329
1033330
1033331
1033332
1033333
1033334
1033335
1033336
1033337
1033338
1033339
10333310
10333311
10333312
10333313
10333314
10333315
10333316
10333317
10333318
10333319
10333320
10333321
10333322
10333323
10333324
10333325
10333326
10333327
10333328
10333329
10333330
10333331
10333332
10333333
10333334
10333335
10333336
10333337
10333338
10333339
103333310
103333311
103333312
103333313
103333314
103333315
103333316
103333317
103333318
103333319
103333320
103333321
103333322
103333323
103333324
103333325
103333326
103333327
103333328
103333329
103333330
103333331
103333332
103333333
103333334
103333335
103333336
103333337
103333338
103333339
1033333310
1033333311
1033333312
1033333313
1033333314
1033333315
1033333316
1033333317
1033333318
1033333319
1033333320
1033333321
1033333322
1033333323
1033333324
1033333325
1033333326
1033333327
1033333328
1033333329
1033333330
1033333331
1033333332
1033333333
1033333334
1033333335
1033333336
1033333337
1033333338
1033333339
10333333310
10333333311
10333333312
10333333313
10333333314
10333333315
10333333316
10333333317
10333333318
10333333319
10333333320
10333333321
10333333322
10333333323
10333333324
10333333325
10333333326
10333333327
10333333328
10333333329
10333333330
10333333331

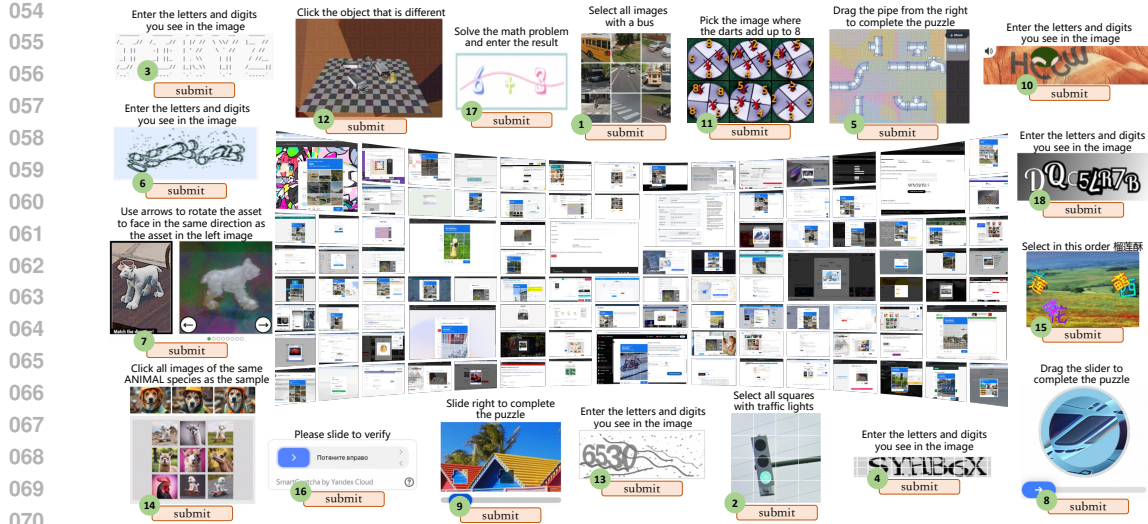


Figure 2: MirrorCAPTCHA filters 2095 valid websites with deployed CAPTCHAs from Common Crawl, covering 18 categories and 1000 puzzle samples, reflecting real-world CAPTCHA distribution.

visual challenges, such as grid selection, character recognition, and slider puzzles, remains an essential capability for their widespread deployment. Crucially, it remains unclear whether current agents can crack complex CAPTCHA in the wild with human-level speed and accuracy.

Mainstream web agent benchmarks (e.g., VisualWebArena (Koh et al., 2024), AgentBench (Liu et al., 2024), and ST-WebAgentBench (Levy et al., 2025)) simulate real online environments but often omit prevalent CAPTCHA challenges. While recent works have introduced CAPTCHA-specific benchmarks, notable limitations persist. For instance, Open CaptchaWorld (Luo et al., 2025) introduces the first interaction-based benchmark but is limited by an extremely small dataset size, which fails to reflect real-world distributions and omits common Optical Character Recognition (OCR) puzzles. MCA-Bench (Wu et al., 2025) constructs a larger-scale, synthetic, homogeneous dataset that lacks practical realism, and some CAPTCHA types lack sufficient complexity, making accurate assessment of agent capabilities in the wild difficult.

To address these issues, we develop **MirrorCAPTCHA**, a benchmark designed to be a “mirror” of real-world CAPTCHA distribution and to accurately assess web agents’ practical automation abilities. We filter out 2095 valid websites with active CAPTCHA puzzles from Common Crawl (Crawl, 2007), then classify them into 18 distinct categories, which comprise 1000 unique puzzles that span various deep learning and web interaction tasks, as shown in Figure 2. Notably, different CAPTCHA types are characterized by distinct frequency distributions, which are statistically derived through random walks on the web subgraph extracted from Common Crawl until a stable state is achieved. This ensures higher-frequency CAPTCHA types are assigned a larger weight in the evaluation. Consequently, the strong performance of an agent on MirrorCAPTCHA indicates its potential effectiveness in real-world scenarios.

Beyond the standard *Weighted Pass Rate* metric, we introduce a customized *Completion Degree* metric for part of the CAPTCHA types. While the pass rate measures binary success, the *Completion Degree* quantifies the “degree” to which an agent “solves” a CAPTCHA, offering a more nuanced measure of its reliability. All puzzles are tested on interactive webpages, as shown in Figure 1, to fully simulate the real-world scenarios agents encounter. Agents must perceive screenshots and perform actions like clicking, pressing keys, and dragging elements until the task is complete.

Additionally, we develop a lightweight and scalable data synthetic pipeline to train a model, Ovis2-Agent-CAPTCHA-8B. This model is trained on 370k synthetic CAPTCHA samples. Experiments on MirrorCAPTCHA show that Ovis2-Agent-CAPTCHA-8B significantly outperforms state-of-the-art closed-source models. For instance, on the high-traffic “Patch Select” category, our model surpasses Gemini-2.5-Pro by 30.66% in *Weighted Pass Rate*. The model’s strong performance on both new metrics, including a high score in *Completion Degree* on challenging puzzles, highlights its potential for real-world web automation and sets a new state-of-the-art for multimodal agents on CAPTCHA challenges.

108

2 RELATED WORKS

109
 110 **Web Agents.** Web Agents (Gur et al., 2024; He et al., 2024; Lai et al., 2024; Agashe et al., 2025;
 111 Huq et al., 2025; Shao et al., 2025; Erdogan et al., 2025), built upon large foundation models (Dubey
 112 et al., 2024; Yang et al., 2025), are designed to simulate human behavior and automate repetitive web
 113 tasks. These agents typically follow a three-step pipeline: perception (interpreting visual information
 114 from screenshots and text), planning/reasoning (decomposing tasks and generating actions), and
 115 execution (localizing elements and performing interactions). Recent advances, such as Auto-
 116 GPT (Significant Gravitas, 2023), demonstrate the ability to handle complex tasks with minimal
 117 user interaction. Similarly, multimodal agents like WebVoyager (He et al., 2024) and MMAC-
 118 Copilot (Song et al., 2024) leverage advanced models like GPT-4V (Yang et al., 2023) and Gemini
 119 Vision (Anil et al., 2023) to process diverse inputs, including screenshots and video content. Train-
 120 ing strategies for these agents encompass data preprocessing, augmentation, and various fine-tuning
 121 methods, all of which aim to improve their end-to-end performance.
 122

123 **Captcha Benchmarks and Models.** The development of deep learning has significantly advanced
 124 CAPTCHA recognition. Early methods relied on convolutional neural networks (CNNs) for feature
 125 extraction (Thobhani et al., 2020; Tang, 2024), while subsequent work combined CNNs and
 126 recurrent neural networks (RNNs) to handle variable-length CAPTCHA sequences (Hu et al., 2018;
 127 Dereia et al., 2023). Generative adversarial networks (GANs) had also been used to synthesize large
 128 datasets for training CAPTCHA-cracking models (Shu & Xu, 2019; Ye et al., 2020). However,
 129 these models are often style-specific and lack the generalization required for real-world CAPTCHA
 130 variants. Existing benchmarks suffer from similar limitations. BeCAPTCHA-Mouse, for exam-
 131 ple, focuses on mouse trajectories with synthetic types, while Open CaptchaWorld (Luo et al.,
 132 2025) omits common Optical Character Recognition (OCR) CAPTCHA and has a small data size.
 133 MCA-Bench (Wu et al., 2025) evaluates vision-language models against synthetic, homogeneous
 134 CAPTCHA puzzles that do not reflect the diversity and complexity of real-world challenges. This
 135 gap, caused by a lack of benchmarks grounded in real-world distributions, prevents an accurate
 136 assessment of web agents’ practical CAPTCHA-solving performance.
 137

138

3 MIRRORCAPTCHA

139 MirrorCAPTCHA is a carefully curated benchmark of real-world CAPTCHA puzzles that are chal-
 140 lenging for agents but easily solvable for humans. Most of the puzzles are directly collected from
 141 real websites and manually annotated, with a small portion sourced from MCA-Bench. The bench-
 142 mark is evaluated using two metrics: *Weighted Pass Rate* (WPR) and a newly introduced metric,
 143 *Completion Degree* (CD), which applies to a fraction of CAPTCHA types.
 144

145

3.1 DESKTOP WEB CURATION

146 MirrorCAPTCHA focuses on web agents that browse on desktop computers. To this end, the
 147 first step is to collect a large list of commonly visited, accessible desktop websites. Common
 148 Crawl (Crawl, 2007) provides a web graph of global internet traffic spanning the past six months,
 149 comprising 156.1 million nodes and 2.1 billion edges. Each node denotes a website accessed from a
 150 specific device (e.g., desktop computer, phone), and each edge corresponds to a browsing transition.
 151

152 From this graph, we select the top 15,000 nodes based on degree as initial candidate sites. We
 153 then use a modified version WebVoyager (He et al., 2024) to query Claude-4-Sonnet for
 154 assessing their accessibility, filtering out inaccessible webpages (see Figure 3, top). The resulting
 155 corpus comprises 10,000 valid websites spanning diverse domains, including entertainment, media,
 156 and social network platforms.
 157

158

3.2 CAPTCHA-CONFRONTED WEB CURATION

159 The next step is to identify websites that trigger CAPTCHA mechanisms. Standard user actions (e.g.,
 160 direct registration or login by users) often do not trigger CAPTCHA, as such actions are typically
 161 not flagged as suspicious. Therefore, we deploy autonomous agents to systematically navigate and
 162 interact with registration and authentication workflows. This approach both increases the likelihood
 163 of triggering CAPTCHA challenges and reflects real-world challenges faced by web agents.
 164

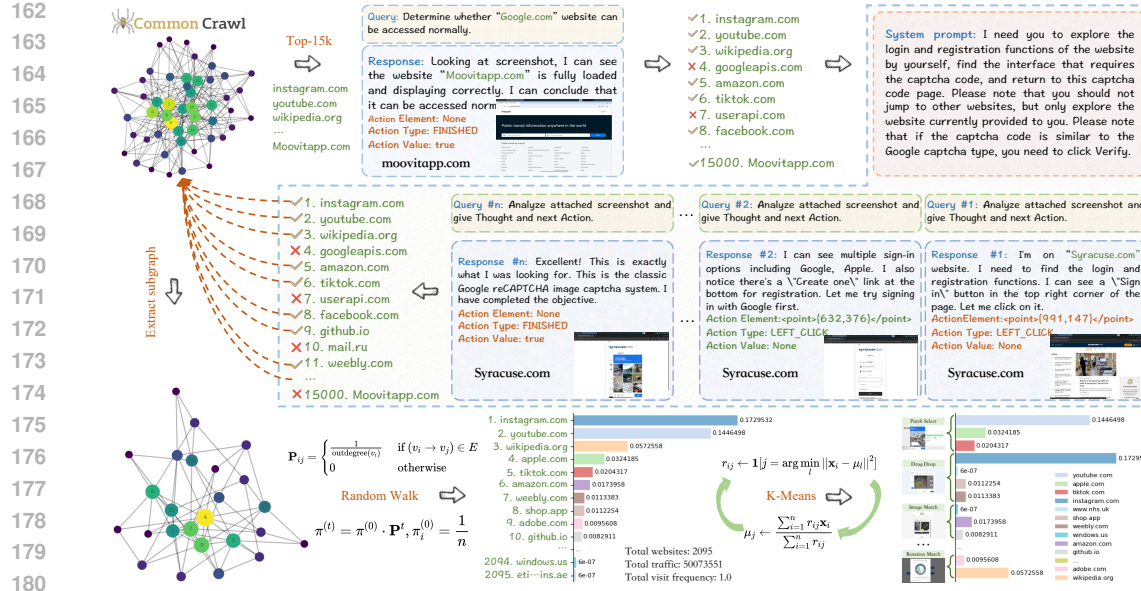


Figure 3: MirrirCAPTCHA construction pipeline. Top: modified WebVoyager querying Claude-4-Sonnet about website accessibility. Middle: Claude-4-Sonnet autonomously explores website functionalities that may trigger CAPTCHA (e.g., registration, login, password reset, account recovery). Termination occurs when a CAPTCHA is triggered, the step limit is reached, or no CAPTCHA is confirmed. Bottom left: random walk for access probability estimation. Bottom right: K-means clustering for CAPTCHA categorization.

Figure 3 (middle) illustrates the entire free exploration process. We observe that if the agent fails to trigger a CAPTCHA on the current website, it will randomly navigate to other sites to continue searching for CAPTCHA challenges. Agents tend to force the completion of tasks regardless of the rationality of their execution. To mitigate this, we impose behavioral constraints:

- *Restricting exploration to registration/login interfaces*
- *Prohibiting site navigation beyond the given website*
- *Prioritizing interactions with web elements that could trigger CAPTCHA*

These rules ensure reliable activation and prevent redundancy. From the 10,000 valid websites, we identify 2,095 websites with CAPTCHAs deployed spanning multiple languages (English, Chinese, Russian), and diverse puzzle types (image/patch recognition, OCR, slides, drag-and-drop, arithmetic, and semantic tasks). While intuitive for humans, these puzzles remain difficult for agents.

Another critical consideration is that the real-world encounter frequency of a specific CAPTCHA type is directly determined by the traffic of websites that host it. For example, high-traffic platforms (e.g., Google, Facebook, YouTube), moderately popular niche sites with relatively lower traffic (e.g., GitHub, Adobe), and numerous obscure small websites with minimal traffic. Therefore, to accurately model the probability of a web agent encountering a particular CAPTCHA type, the benchmark must account for the traffic variations among the websites that deploy it.

3.3 WEB AND CAPTCHA ACCESS PROBABILITIES

To simulate real jumping behavior among websites, we perform random walks on the subgraph extracted from Common Crawl. Extracting nodes and edges adjacent to the 2,095 websites yields a connected subgraph \mathcal{G}_s with 15 million nodes and 75 million edges. Let $\mathbb{V} := \{v_1, v_2, \dots, v_n\}$ denote its node set and $\mathbb{E} := \{e_1, e_2, \dots, e_m\}$ denote its edge set. We define the transition matrix:

$$P_{ij} = \begin{cases} \frac{1}{\text{outdegree}(v_i)} & \text{if } (v_i \rightarrow v_j) \in \mathbb{E}, \\ 0 & \text{otherwise,} \end{cases} \quad (1)$$

where $\text{outdegree}(v_i)$ denotes the number of outgoing edges from the node v_i . We initialize the visit probability distribution uniformly over the entire node set \mathbb{V} :

$$\pi_i^{(0)} = \frac{1}{n}, \quad \forall i = 1, 2, \dots, n. \quad (2)$$

216 After t steps, the node visit distribution is given by $\pi^{(t)} = \pi^{(t-1)} \cdot \mathbf{P}$. Recursively, we obtain
 217 $\pi^{(t)} = \pi^{(0)} \cdot \mathbf{P}^t$, with $\pi_i^{(t)}$ representing the probability of being at node v_i after t steps. After 10^8
 218 steps (the cutoff used in our study), the final visit probability distribution is:
 219

$$\pi^{(10^8)} = \pi^{(0)} \cdot \mathbf{P}^{10^8}, \quad (3)$$

220 where $\pi_i^{(10^8)}$ is the probability of visiting node v_i . The bottom-left panel of Figure 3 illustrates
 221 the resulting traffic distribution, where a handful of high-traffic websites (e.g., `instagram.com`,
 222 `youtube.com`, `wikipedia.org`) account for nearly half of all visits, and thus half of
 223 CAPTCHA encounters. *Detailed visit probability distribution \mathbb{V} is provided in Appendix C.*
 224

225 Next, we categorize CAPTCHA types into clusters by applying K-means clustering. For each
 226 website screenshot w_i , we extract the CLIP (Radford et al., 2021) image embedding $\mathbf{f}_i \in \mathbb{R}^d$:
 227

$$\mathbf{f}_i = \phi(w_i), \quad d = 512, \quad (4)$$

228 and stack the vectors to form:
 229

$$\mathbf{F} = [\mathbf{f}_1, \mathbf{f}_2, \dots, \mathbf{f}_N]^\top \in \mathbb{R}^{N \times d}, \quad N = 2095. \quad (5)$$

230 We then apply K-means to partition \mathbf{F} into K clusters $\{C_1, C_2, \dots, C_K\}$ via the standard iterative
 231 assignment-and-update procedure:
 232

$$\begin{aligned} r_{ij} &\leftarrow \mathbf{1} \left[j = \arg \min_l \|\mathbf{f}_i - \boldsymbol{\mu}_l\|^2 \right], \\ \boldsymbol{\mu}_j &\leftarrow \frac{\sum_{i=1}^N r_{ij} \mathbf{f}_i}{\sum_{i=1}^N r_{ij}}, \end{aligned} \quad (6)$$

233 where $\boldsymbol{\mu}_j$ denotes the centroid of cluster C_j , and r_{ij} is an indicator of whether w_i belongs to C_j .
 234 Starting from $K = 2$, we iteratively refine the clustering, manually examine the clustering results,
 235 and further partition more fine-grained clusters. Ultimately, we obtain 18 distinct CAPTCHA types,
 236 as shown in the bottom-right panel in Figure 3.
 237

238 Once the clustering is completed, we compute the visit probability of each CAPTCHA category C_j
 239 by aggregating the visit probability $\pi_i^{(10^8)}$ of all websites in that cluster:
 240

$$p(C_j) = \sum_{w_i \in C_j} \pi_i^{(10^8)}, \quad j = 1, 2, \dots, K. \quad (7)$$

241 The resulting distribution of access frequencies across the 18 CAPTCHA categories is summarized
 242 in Table 1, where the categories show a heavy-tailed pattern – a few dominant types (such as dis-
 243 torted alphanumeric text or simple image-based challenges) account for the majority of real-world
 244 traffic, whereas many others are far less prevalent. This skewed distribution will directly impact the
 245 design of evaluation datasets and robustness benchmarks for automated CAPTCHA solvers.
 246

247 The final step is to construct puzzle samples for each CAPTCHA type in proportion to visit fre-
 248 quency: categories with higher traffic are allocated more samples, thereby mirroring real-world
 249 CAPTCHA distribution patterns. However, some categories (e.g., OCR Gradient, Type Arithmetic)
 250 exhibit extremely low traffic. For instance, in a benchmark with 1,000 samples, OCR Gradient
 251 would yield only 1-2 puzzles ($1,000 \times 0.00148$), which is overly sparse. Conversely, Image Recog-
 252 nition or Patch Selection may dominate with hundreds of samples, leading to redundancy.
 253

254 To balance realism and robustness, we cap the number of samples per category at 50 or 100, as shown
 255 in Table 1. See Appendix A for the comparison with OpenCaptchaWorld and MCA-Bench. During
 256 evaluation, the true visit frequencies remain as weights when aggregating results, ensuring that the
 257 *Weighted Pass Rate* reflects real-world CAPTCHA distribution while avoiding extreme sparsity or
 258 overrepresentation. Details of this measure strategy are discussed in the following subsection.
 259

260 3.4 EVALUATION METRICS

261 MirrorCAPTCHA employs two metrics: *Weighted Pass Rate* (WPR) and *Completion Degree* (CD).
 262 WPR measures whether a model fully solves a CAPTCHA puzzle, weighted by real-world encounter
 263 probabilities, and CD quantifies how close a model comes to a full solution. All CAPTCHA types
 264 can be assessed with WPR, whereas only a subset is compatible with it. For example, Image Match
 265 puzzles are strictly binary (match or non-match) and therefore can only be evaluated using WPR.
 266

270 Table 1: Statistics of the MirrorCAPTCHA benchmark by category, including website coverage, visit traffic,
 271 relative frequency, example puzzles, task description, and number of samples. Categories are ordered by traffic:
 272 1. Image Recognition, 2. Patch Select, 3. OCR Grey, 4. OCR Grid, 5. Drag Drop, 6. OCR ColorPure, 7. Image
 273 Match, 8. Rotation Match, 9. Slide Puzzle, 10. OCR ColorPattern, 11. Semantic Select, 12. Semantic Area,
 274 13. OCR Dot, 14. Reference Match, 15. Click Order, 16. Slide Line, 17. Type Arithmetic, 18. OCR Gradient.

Type name	Covered	Traffic	Frequency	CAPTCHA description	Samples
Image Recognition	652	17961686	0.35871	Identify target objects grid in a 9-image grid	100
Patch Select	709	17449069	0.34847	Identify target objects patches in a 16-image grid	100
OCR Grey	95	4594340	0.09175	OCR: grayscale text, and line noise	50
OCR Grid	22	1798535	0.03592	OCR: grayscale text, grid background, and line noise	50
Drag Drop	58	1465736	0.02927	Drag small image to correct position on large image	50
OCR ColorPure	159	1408947	0.02814	OCR: color font, pure background, and color line noise	50
Image Match	18	1094478	0.02186	Select matching image from candidates based on reference	50
Rotation Match	6	1047564	0.02092	Rotate tile to correct position via slider	50
Slide Puzzle	103	811840	0.01621	Slide puzzle piece to correct position	50
OCR ColorPattern	46	428499	0.00856	OCR: color font, pattern background, and color line noise	50
Semantic Select	50	516790	0.01032	Select images from 3x3 grid following instructions	50
Semantic Area	34	514516	0.01027	Select the different icon from multiple similar ones	50
OCR Dot	57	248757	0.00497	OCR: grayscale text, pockmarked background, and line noise	50
Reference Match	26	209916	0.00419	Select from 3x3 grid based on references and instructions	50
Click Order	15	182529	0.00365	Click icons in specified sequence	50
Slide Line	13	159555	0.00319	Slide block to endpoint	50
Type Arithmetic	15	106586	0.00213	Solve arithmetic problem and enter result	50
OCR Gradient	17	74208	0.00148	OCR: grayscale font, gradient background, and line noise	50
Total	2095	50073551	1.0	–	1000

294
 295 **Weighted Pass Rate (WPR).** The visit probability $p(C_j)$ of a given CAPTCHA category is de-
 296 fined in Equation 7. Let N_i denote the total number of puzzle samples in category i , and S_i denote
 297 the number of puzzles that the model fully and correctly solves. Then:

$$298 \quad \mathbf{WPR} = \sum_{i=1}^k \left(p_i \times \frac{S_i}{N_i} \right) \times 100\% \quad (8)$$

301
 302 **Completion Degree (CD).** CD is defined for 12 categories using 4 task-specific measures (See
 303 Appendix B for detailed evaluation metrics):

- 304 • F1 score (van Rijsbergen, 1979): Applied to Image Recognition, Patch Select, Semantic
 305 Select, and Reference Match; computes the F1 score between model predictions and ground
 306 truth labels.
- 307 • Levenshtein Distance (Levenshtein, 1966): Applied to OCR Grey, OCR Gradient,
 308 OCR Grid, OCR ColorPure, OCR ColorPattern, and OCR Dot; measures edit distance
 309 between predicted and true strings.
- 310 • Sequence Matching: Applied to Click Order; counts one-to-one matches between the
 311 predicted and ground truth sequences.
- 312 • Angle Distance: Applied to Rotation Match; measures angular difference between
 313 predicted and ground truth orientations.

315 Taken together, WPR and CD offer a holistic evaluation of CAPTCHA-solving performance, cap-
 316 turing both strict accuracy and partial progress.

318 4 OVIS2-AGENT-CAPTCHA-8B

321 Unlike prior deep learning models that target a single CAPTCHA type (e.g., 3×3 or 4×4 grids) with
 322 task-specific designs, the MirrorCAPTCHA benchmark evaluates the broader capability of MLLM-
 323 based web agents to solve diverse, real-world CAPTCHAs. This naturally raises the question: *how
 can we enhance a web agent’s ability to generalize across a wide range of CAPTCHA types?*

To address this, we design a lightweight, extensible CAPTCHA synthesis pipeline in Figure 4 that can automatically generate puzzles by defining certain rules for data organization. Leveraging this synthesized data, we apply supervised fine-tuning (SFT) to Ovis2-8B (Lu et al., 2024), yielding Ovis2-Agent-CAPTCHA-8B. Ovis2-Agent-CAPTCHA-8B is trained with SFT on 370k synthesized CAPTCHA samples (including Image Recognition, Patch Select, Semantic Area, OCR, and Type Arithmetic types), augmented with limited computer-use trajectory data to improve cross-scenario adaptability. Training requires 35 hours on 64 H100 GPUs, enabling the model to acquire the necessary skills in visual grounding, semantic reasoning, and interactive operation for CAPTCHA solving.

We then benchmark the model against both open-source and closed-source counterparts. Experimental results show that Ovis2-Agent-CAPTCHA-8B not only surpasses existing open-sourced models but also significantly outperforms state-of-the-art closed-sourced systems on MirrorCAPTCHA, setting a new technical baseline for CAPTCHA-solving agents.

5 EXPERIMENTS ANALYSIS

5.1 EXPERIMENTAL SETUP

We systematically evaluate both browser-use agents and computer-use agents, each equipped with different MLLM backbones, on the MirrorCAPTCHA benchmark. To ensure fairness, we adopt consistent prompting strategies and uniform evaluation metrics across all models. **Browser-use agents**, implemented with the set-of-mark (SOM) paradigm (Müller & Žunić, 2024), include OpenAI o4-mini (OpenAI, 2025), Gemini-2.5-Pro (Anil et al., 2023), Claude-4-Sonnet (Anthropic, 2025), and GPT-4.1 (OpenAI, 2025). **Computer-use agents** are deployed via the augmented Web-Voyager framework (He et al., 2024), covering Claude-4-Sonnet (Anthropic, 2025), UI-TARS-72B-DPO (Qin et al., 2025), and our Ovis2-Agent-CAPTCHA-8B model.

Table 2: WPR on MirrorCAPTCHA for Browser-Use (OpenAI o4-mini, Gemini-2.5-Pro, Claude-4-Sonnet, GPT-4.1) and Computer-Use Agents (Claude-4-Sonnet, UI-TARS-72B-DPO, Ovis2-Agent-CAPTCHA-8B).

CAPTCHA Type	Browser-Use Agent				Computer-Use Agent		
	o4-mini	Gemini-2.5-Pro	Claude-4-Son	GPT-4.1	Claude-4-Son	UI-TARS	Ovis2-8B
Image Recognition	53.87	64.33	3.72	47.67	35.33	40.07	66.67
Patch Select	14.72	14.67	2.76	4.67	10.00	5.39	45.33
OCR Grey	50.00	62.00	30.00	54.00	38.00	48.00	54.00
OCR Grid	36.00	54.00	20.00	44.00	22.00	37.50	52.00
Drag Drop	0.00	0.00	0.00	0.00	0.00	0.00	0.00
OCR ColorPure	44.00	62.00	24.00	54.00	32.00	40.00	50.00
Image Match	6.67	31.03	14.29	13.33	30.00	23.33	6.67
Rotation Match	0.00	0.00	0.00	0.00	0.00	4.00	0.00
Slide Puzzle	0.00	0.00	0.00	0.00	0.00	4.00	0.00
OCR ColorPattern	62.00	74.00	28.00	64.00	32.00	52.00	60.00
Semantic Select	30.00	56.67	24.21	43.33	46.67	33.33	26.67
Semantic Area	0.00	0.00	0.00	0.00	40.00	53.33	16.67
OCR Dot	50.00	70.00	32.00	54.00	30.00	50.00	74.00
Reference Match	50.00	83.33	33.33	33.33	0.00	23.33	10.00
Click Order	0.00	0.00	0.00	0.00	0.00	3.75	<u>1.25</u>
Slide Line	0.00	0.00	0.00	0.00	50.00	80.00	20.00
Type Arithmetic	93.33	96.67	90.00	90.00	90.00	80.00	96.67
OCR Gradient	64.00	70.00	34.00	62.00	40.00	60.00	<u>64.00</u>
Average	33.66	<u>40.22</u>	7.77	28.58	23.58	25.85	49.57

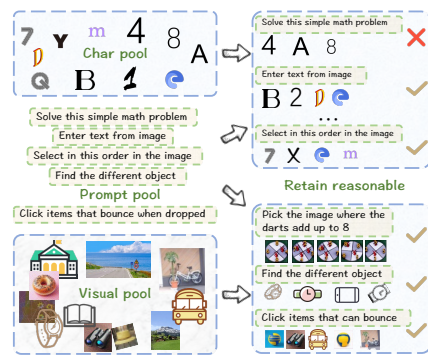


Figure 4: Synthesize CAPTCHA pipeline.

378
379

5.2 WEIGHTED PASS RATE AND COMPLETION DEGREE

380
381
382
383
384
385

Table 2 reports the WPR for all models. Due to inherent limitations of the browser-use execution framework (Müller & Žunić, 2024), such agents cannot perform operations like “Drag Drop”, “Rotation match”, “Slide Puzzle”, “Semantic Area”, “Click Order” or “Slide Line”. Specifically, the SOM mechanism treats an image as a single object and cannot localize or manipulate elements within it. By contrast, computer-use agents directly simulate mouse interactions, enabling them to attempt all CAPTCHA categories.

386
387
388
389
390
391

Weighted Pass Rate. Ovis2-Agent-CAPTCHA-8B achieves the highest average WPR. Notably, on the high-traffic “Patch Select” category, it surpasses Gemini by 30.66 percentage points. For Claude-4-Sonnet (computer-use), WPR drops to zero in some categories, largely due to sensitivity to image resolution, which prevents reliable coordinate output for click actions. For Claude-4-Sonnet (browser-use), failures in “Image Recognition” and “Patch Select” stem from repeated memory read/write loops, reflecting a fundamental vulnerability of the framework.

392
393
394

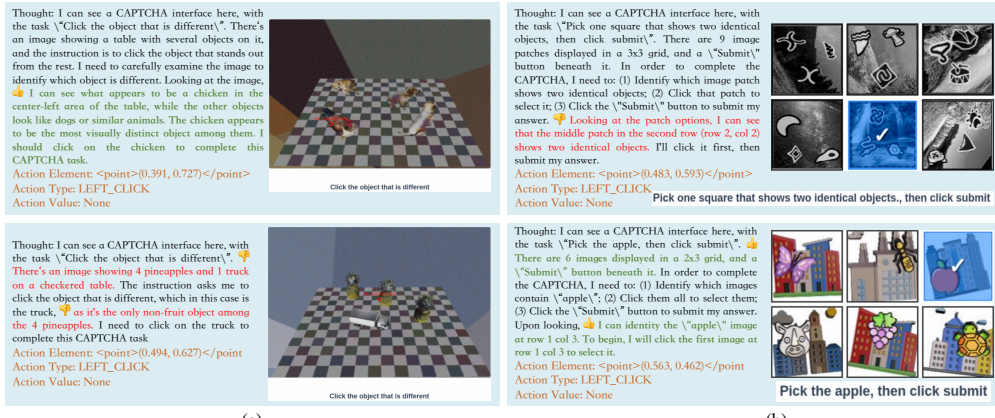
Table 3: CD on MirrorCAPTCHA for Browser-Use (OpenAI o4-mini, Gemini-2.5-Pro, Claude-4-Sonnet, GPT-4.1) and Computer-Use Agents (Claude-4-Sonnet, UI-TARS-72B-DPO, Ovis2-Agent-CAPTCHA-8B).

395
396
397
398
399
400
401
402
403
404
405
406
407
408
409

CAPTCHA Type	Browser-Use Agent				Computer-Use Agent		
	o4-mini	Gemini-2.5-Pro	Claude-4-Son	GPT-4.1	Claude-4-Son	UI-TARS	Ovis2-8B
Image Recognition	84.27	80.88	22.83	66.77	76.22	72.11	89.66
Patch Select	72.82	70.22	33.49	57.53	61.60	57.24	88.14
OCR Grey	81.53	84.52	65.84	82.52	70.41	76.08	78.84
OCR Grid	76.13	84.69	56.21	78.56	60.26	72.68	78.10
OCR ColorPure	75.66	85.30	62.15	81.41	67.47	75.60	79.14
Rotation Match	0.00	0.00	0.00	0.00	0.00	60.97	60.27
OCR ColorPattern	85.20	89.83	64.52	86.20	68.26	76.15	79.53
Semantic Select	49.48	<u>62.22</u>	31.11	64.32	60.37	55.95	61.25
OCR Dot	76.00	89.23	60.54	82.85	67.78	77.49	<u>88.33</u>
Reference Match	<u>69.68</u>	89.44	39.32	58.97	0.00	55.95	49.27
Click Order	0.00	0.00	0.00	0.00	0.00	11.46	<u>10.62</u>
OCR Gradient	85.63	<u>85.63</u>	65.15	89.33	71.41	82.54	84.36
Average	63.03	<u>68.50</u>	41.68	62.37	50.32	64.52	70.63

410
411
412
413
414
415

Completion Degree. Table 3 shows that Ovis2-Agent-CAPTCHA-8B also achieves the best average CD. Interestingly, in categories such as “Patch Select”, the WPR is relatively low across all models, while CD remains high, indicating that models select most patches correctly but often fail to complete the task perfectly. This suggests that higher image resolution, more query steps, or finer-grained behavioral optimization could close the gap between CD and WPR.

416
417
418
419
420
421
422
423
424
425
426
427
428
429
430

431

Figure 5: Correct vs. error cases for Ovis2-Agent-CAPTCHA-8B on (a) “Click the object that is different” and (b) “Semantic Select”.

432
433

5.3 SUCCESS AND FAILURE CASE ANALYSIS

434
435
436
437
438
439

Figure 5 presents typical success and failure cases. In the correct case of the “Click the object that is different” task, the model identifies a chicken among dog-like animals and clicks the correct location. In the error case, however, it misclassifies the objects as 4 pineapples and 1 truck. Although it correctly identifies the truck as the outlier, the click misses the precise coordinates, causing task failure. Similarly, in the error case, failure arises from difficulty in interpreting abstract icons. Here, the model guesses randomly rather than reasoning about semantic differences.

440
441
442
443

These cases highlight two key limitations: (i) imprecise visual recognition of object attributes and counts, and (ii) difficulty in extracting discriminative features from abstract images. Addressing these issues will require improved visual feature extraction and more reliable object classification.

444
445
446
447
448
449
450
451
452
453

5.4 INFERENCE PROCESS ON CHALLENGING CAPTCHA PUZZLES

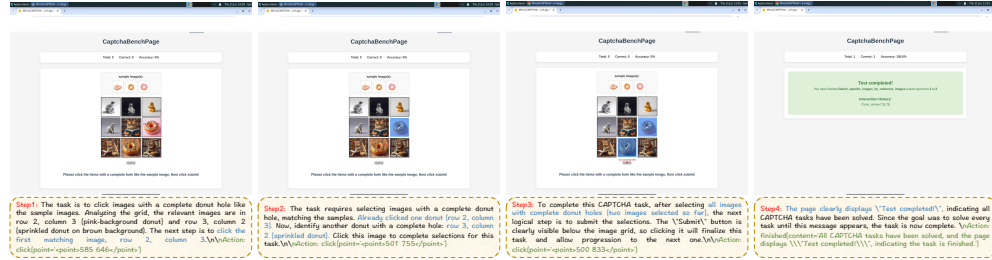
454
455

Figure 6: CAPTCHA puzzle: Click the items with a complete hole, as shown in the sample images.

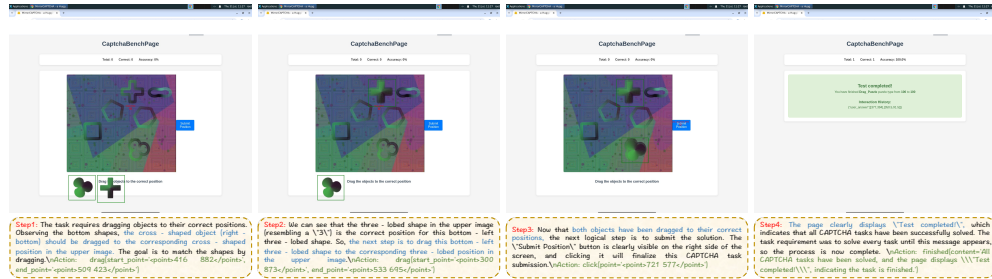
456
457
458
459
460
461
462
463
464465
466

Figure 7: CAPTCHA puzzle: Drag the objects to their correct position.

467
468
469
470
471
472
473
474
475

Figures 6 and 7 provide a qualitative look into how web agent solves challenging CAPTCHA on the MirrorCAPTCHA benchmark. First, it accurately interprets the natural language instructions provided by the puzzle, such as identifying the required criteria (“items with a complete hole”) or understanding the action needed (“Drag the objects to their correct position”). The agent then applies its visual reasoning skills to identify the correct target elements on the webpage. Finally, it translates this understanding into a series of precise interactive operations, including clicks, drags, and text entry, to complete the CAPTCHA task. This seamless integration of perception, reasoning, and execution highlights the agent’s advanced capabilities. *More detailed examples of the agent’s reasoning process are provided in Appendix D.*

476
477

6 CONCLUSION

478
479
480
481
482
483
484
485

We present **MirrorCAPTCHA**, a benchmark designed to act as a “mirror” of real-world CAPTCHA distributions. It filters 2,095 valid websites with deployed CAPTCHAs from Common Crawl, categorized into 18 types spanning both deep learning and web interaction tasks. To approximate real-world encounter frequencies, MirrorCAPTCHA employs random walks and evaluates performance using two metrics: *Weighted Pass Rate* and *Completion Rate*. In addition, we introduce *Ovis2-Agent-CAPTCHA-8B*, a model trained on a synthesized CAPTCHA dataset. Experimental results show that it significantly outperforms both open-source and closed-source counterparts, surpassing Gemini-2.5-Pro by 9.4% in Weighted Pass Rate and achieves the highest Completion Degree across most CAPTCHA categories.

486 REFERENCES
487

488 Saaket Agashe, Jiuzhou Han, Shuyu Gan, Jiachen Yang, Ang Li, and Xin Eric Wang. Agent s: An
489 open agentic framework that uses computers like a human. In *ICLR*, 2025.

490 Rohan Anil, Sebastian Borgeaud, Yonghui Wu, Jean-Baptiste Alayrac, Jiahui Yu, Radu Soricut,
491 et al. Gemini: A family of highly capable multimodal models. In *arXiv*, 2023.

492 Anthropic. Claude api, 2025. URL <https://www.anthropic.com/api>. Anthropic’s Con-
493 versational AI API.

494 Zhe Chen, Weiyun Wang, Yue Cao, Yangzhou Liu, Zhangwei Gao, Erfei Cui, et al. Expanding per-
495 formance boundaries of open-source multimodal models with model, data, and test-time scaling.
496 In *arXiv*, 2024.

497 Common Crawl. Common crawl, 2007. URL <https://commoncrawl.org/>. Common Crawl
498 corpus contains petabytes of data, regularly collected since 2008.

499 Zaid Dereia, Beiji Zou, Amal A. Al-Shargabi, Alaa Thobhani, and Amr Abdussalam. Deep learning
500 based CAPTCHA recognition network with grouping strategy. *Sensors*, 23(23):9487, 2023.

501 Abhimanyu Dubey, Abhinav Jauhri, Abhinav Pandey, Abhishek Kadian, Ahmad Al-Dahle, Aiesha
502 Letman, et al. The llama 3 herd of models. In *arXiv*, 2024.

503 Lutfi Eren Erdogan, Nicholas Lee, Sehoon Kim, Suhong Moon, Hiroki Furuta, Gopala Anu-
504 manchipalli, Kurt Keutzer, and Amir Gholami. Plan-and-act: Improving planning of agents for
505 long-horizon tasks. In *arXiv*, 2025.

506 Izzeddin Gur, Hiroki Furuta, Austin V. Huang, Mustafa Safdari, Yutaka Matsuo, Douglas Eck, and
507 Aleksandra Faust. A real-world webagent with planning, long context understanding, and pro-
508 gram synthesis. In *ICLR*, 2024.

509 Hongliang He, Wenlin Yao, Kaixin Ma, Wenhao Yu, Yong Dai, Hongming Zhang, Zhenzhong Lan,
510 and Dong Yu. Webvoyager: Building an end-to-end web agent with large multimodal models. In
511 *ACL*, pp. 6864–6890, 2024.

512 Yu Hu, Li Chen, and Jun Cheng. A captcha recognition technology based on deep learning. In
513 *ICIEA*, pp. 617–620, 2018.

514 Faria Huq, Zora Zhiruo Wang, Frank F. Xu, Tianyue Ou, Shuyan Zhou, Jeffrey P. Bigham, and
515 Graham Neubig. Cowpilot: A framework for autonomous and human-agent collaborative web
516 navigation. In *arXiv*, 2025.

517 Jing Yu Koh, Robert Lo, Lawrence Jang, Vikram Duvvur, Ming Chong Lim, Po-Yu Huang, Gra-
518 ham Neubig, Shuyan Zhou, Russ Salakhutdinov, and Daniel Fried. Visualwebarena: Evaluating
519 multimodal agents on realistic visual web tasks. In *ACL*, pp. 881–905, 2024.

520 Hanyu Lai, Xiao Liu, Iat Long Iong, Shuntian Yao, Yuxuan Chen, Pengbo Shen, Hao Yu, Hanchen
521 Zhang, Xiaohan Zhang, Yuxiao Dong, and Jie Tang. Autowebglm: A large language model-based
522 web navigating agent. In *KDD*, pp. 5295–5306, 2024.

523 Vladimir I. Levenshtein. Binary codes capable of correcting deletions, insertions, and reversals.
524 *Soviet Physics Doklady*, 10(8):707–710, 1966.

525 Ido Levy, Ben Wiesel, Sami Marreed, Alon Oved, Avi Yaeli, and Segev Shlomov. St-
526 webagentbench: A benchmark for evaluating safety and trustworthiness in web agents. In *arXiv*,
527 May 2025.

528 Xiao Liu, Hao Yu, Hanchen Zhang, Yifan Xu, Xuanyu Lei, Hanyu Lai, et al. Agentbench: Evaluat-
529 ing llms as agents. In *ICLR*, 2024.

530 Shiyin Lu, Yang Li, Qing-Guo Chen, Zhao Xu, Weihua Luo, Kaifu Zhang, and Han-Jia Ye. Ovis:
531 Structural embedding alignment for multimodal large language model. In *arXiv*, 2024.

540 Yixin Luo, Zhaoyi Li, Jiacheng Liu, Jiacheng Cui, Xiaohan Zhao, and Zhiqiang Shen. Open
 541 captchaworld: A comprehensive web-based platform for testing and benchmarking multimodal
 542 LLM agents. In *NeurIPS*, 2025.

543

544 Magnus Müller and Gregor Žunič. Browser use: Enable ai to control your browser, 2024. URL
 545 <https://github.com/browser-use/browser-use>.

546 OpenAI. Openai api, 2025. URL <https://openai.com/api/>. Accessed: 2023-12-01.

547

548 Yujia Qin, Yining Ye, Junjie Fang, Haoming Wang, Shihao Liang, Shizuo Tian, et al. Ui-tars:
 549 Pioneering automated GUI interaction with native agents. In *arXiv*, 2025.

550 Alec Radford, Jong Wook Kim, Chris Hallacy, Aditya Ramesh, Gabriel Goh, Sandhini Agarwal,
 551 et al. Learning transferable visual models from natural language supervision. In *ICML*, volume
 552 139, pp. 8748–8763, 2021.

553

554 Chenyang Shao, Xinyuan Hu, Yutang Lin, and Fengli Xu. Division-of-thoughts: Harnessing hybrid
 555 language model synergy for efficient on-device agents. In *WWW*, pp. 1822–1833, 2025.

556 Yujin Shu and Yongjin Xu. End-to-end captcha recognition using deep cnn-rnn network. In *IMCEC*,
 557 pp. 54–58, 2019.

558

559 Significant Gravitas. AutoGPT, 2023. URL <https://agpt.co/>.

560

561 Zirui Song, Yaohang Li, Meng Fang, Zhenhao Chen, Zecheng Shi, Yuan Huang, and Ling Chen.
 562 Mmac-copilot: Multi-modal agent collaboration operating system copilot. In *arXiv*, 2024. URL
 563 <https://doi.org/10.48550/arXiv.2404.18074>.

564

565 Shengyuan Tang. Research on captcha recognition technology based on deep learning. *Applied and
 Computational Engineering*, 81:41–46, 11 2024.

566

567 Alaa Thobhani, Mingsheng Gao, Ammar Hawbani, Safwan Taher Mohammed Ali, and Amr Ab-
 568 dussalam. Captcha recognition using deep learning with attached binary images. *Electronics*, 9
 (9), 2020.

569

570 C. J. van Rijsbergen. Information retrieval. In *Butterworth-Heinemann*, 1979.

571

572 Peng Wang, Shuai Bai, Sinan Tan, Shijie Wang, Zhihao Fan, Jinze Bai, et al. Qwen2-vl: Enhancing
 573 vision-language model’s perception of the world at any resolution. In *arXiv*, 2024.

574

575 Zonglin Wu, Yule Xue, Xin Wei, and Yiren Song. Mca-bench: A multimodal benchmark for evalu-
 ating CAPTCHA robustness against vlm-based attacks. In *arXiv*, 2025.

576

577 An Yang, Anfeng Li, Baosong Yang, Beichen Zhang, Binyuan Hui, Bo Zheng, et al. Qwen3 techni-
 578 cal report. In *arXiv*, 2025.

579

580 Zhengyuan Yang, Linjie Li, Kevin Lin, Jianfeng Wang, Chung-Ching Lin, Zicheng Liu, and Lijuan
 581 Wang. The dawn of lmms: Preliminary explorations with gpt-4v(ision). In *arXiv*, 2023.

582

583 Guixin Ye, Zhanyong Tang, Dingyi Fang, Zhanxing Zhu, Yansong Feng, Pengfei Xu, Xiaojiang
 584 Chen, Jungong Han, and Zheng Wang. Using generative adversarial networks to break and protect
 585 text captchas. *ACM Transactions on Privacy and Security*, 23, 01 2020.

586

587

588

589

590

591

592

593

594 595 596 597 598 599 Appendix for MirrorCAPTCHA

600 A COMPARISON WITH EXISTING CAPTCHA DATASETS

601
602 Table 4: Comparison with Open CaptchaWorld and MCA-Bench benchmarks.

603 Dataset	604 CAPTCHA Distribution	605 Number of Categories	606 Data size	607 CAPTCHA Categories
608 Open CaptchaWorld	609 Random	610 20	611 225	Select Animal, Pick Area, Patch Select, Object Match, Misleading Click, Geometry Click, Image Recognition, Coordinates, Place Dot, Rotation Match, Image Matching, Connect Icon, Bingo, Dart Count, Dice Count, Slide Puzzle, Path Finder, Click Order, Unusual Detection, Hold Button
612 MCA-Bench	613 Random	614 20	615 4,000	616 3×3 Grid Select, 3×3 Jig-swap, Arithmetic Char, Arithmetic Select, Hollow Pattern, Distort Word, Classic Char, Sequential Letter, Bright Dist, Sliding Block, Align Sliders, Rotate Block, Geometry Shape, Rotation Letter, Color Discrimination, Vowel Select, Full-img Grid Select, Text-based Arithmetic, Common Sense, Invert Letter
617 MirrorCAPTCHA	618 Real-world	619 18	620 1,000	621 Image recognition, Patch Select, OCR Grey, OCR Grid, Drag Drop, OCR Color-pure, Image Match, Rotation Match, Slide Puzzle, OCR Color-pattern, Semantic Select, Semantic Area, OCR Dot, Reference Match, CLICK Order, Slide Line, Type Arithmetic, OCR Gradient

622 Table 4 presents a detailed comparison of the three most recent CAPTCHA benchmarks. Both Open
623 CaptchaWorld (Luo et al., 2025) and MCA-Bench (Wu et al., 2025) rely on a random distribution
624 of CAPTCHA types, which fails to accurately reflect the real-world frequencies of these challenges.
625 Open CaptchaWorld includes 20 categories but has an extremely small dataset of just 225 samples,
626 which can lead to high randomness in evaluation. MCA-Bench is larger, with 4,000 samples across
627 20 categories, but its synthetic puzzles do not capture the diversity and complexity found on real
628 websites. In contrast, our MirrorCAPTCHA benchmark is grounded in real-world data. It features
629 18 CAPTCHA types collected from 2,095 live websites, and its distribution is statistically derived
630 from actual web traffic. With a total of 1,000 puzzles, MirrorCAPTCHA provides a more realistic
631 and reliable tool for evaluating web agents, making it a “mirror” that truly reflects an agent’s
632 performance in real-world scenarios.

633 B DETAILED EVALUATION METRIC: COMPLETION DEGREE

634 To capture partial correctness in CAPTCHA-solving tasks, we define Completion
635 Degree (CD) as a family of fine-grained metrics that quantify *how close* a web agent’s output
636 is to the correct answer, even when the CAPTCHA is not fully solved.

637 We adopt four types of CD metrics: F1 Score, Levenshtein Distance, Sequence
638 Matching Accuracy, and Angle Distance Error, each aligned with the nature of spe-
639 cific CAPTCHA categories.

640 ▶ F1 Score

641 This metric is used for puzzles that require selecting one or more items from a set, such as:

- 642 • Image Recognition
- 643 • Patch Select
- 644 • Semantic Select
- 645 • Reference Match

646 **Definition.** The F1 score is the harmonic mean of precision and recall:

$$647 F_1 = \frac{2 \times \text{Precision} \times \text{Recall}}{\text{Precision} + \text{Recall}},$$

648 where

$$649 \text{Precision} = \frac{\text{TP}}{\text{TP} + \text{FP}}, \quad \text{Recall} = \frac{\text{TP}}{\text{TP} + \text{FN}},$$

650 where TP (True Positive) denotes correctly selected items, FP (False Positive) denotes wrongly
651 selected items, and FN (False Negative) denotes missed correct items.

648 **Explanation:** These CAPTCHA types may contain multiple correct elements. F1 score balances
 649 correctness and completeness: selecting wrong patches lowers precision, while missing correct ones
 650 lowers recall. F1 scores are normalized to $[0, 1]$.
 651

652 ▶ Levenshtein Distance

653 This metric is used for CAPTCHAs that involve text recognition:

654

- 655 • OCR Grey
- 656 • OCR Gradient
- 657 • OCR Grid
- 658 • OCR ColorPure
- 659 • OCR ColorPattern
- 660 • OCR Dot

661

662 **Definition.** The Levenshtein distance measures the minimum number of single-character
 663 edits (insertions, deletions, substitutions) needed to transform the predicted string s_1 into the ground
 664 truth s_2 :

$$665 \text{Lev}(s_1, s_2) \in \mathbb{N}^+.$$

666 We convert this distance into a similarity score:

$$667 \text{CD} = 1 - \frac{\text{Lev}(s_1, s_2)}{\max(|s_1|, |s_2|)}.$$

668

669 A score of 1 indicates a perfect match, while a score of 0 indicates completely different strings.
 670

671 **Explanation.** This metric captures OCR-specific errors (e.g., character substitutions) and awards
 672 partial credit when most of the string is correct.

673 ▶ Sequence Matching Accuracy

674 This metric is specifically designed for:

675

- 676 • Click Order

677

678 **Definition.** Let P be the sequence of elements clicked by the agent and G the ground truth sequence.
 679 We compute:

$$680 \text{CD} = \frac{1}{n} \sum_{i=1}^n \mathbf{1}\{P_i = G_i\},$$

681

682 where n is the sequence length, P_i is the i -th clicked element, and $\mathbf{1}\{\cdot\}$ is the indicator function.
 683

684 **Explanation.** This metric measures position-wise accuracy. For example, if the CAPTCHA requires
 685 clicking “Cat → Dog → Bird”, this metric counts how many items are in the correct position. This
 686 allows for partial credit even if the model only gets part of the sequence right.

687 ▶ Angle Distance Error

688 This metric is used for puzzles that require rotation:

689

- 690 • Rotation Match

691

692 **Definition.** Given predicted rotation θ_p and ground truth θ_g , we compute:

$$693 \Delta\theta = \min(|\theta_p - \theta_g|, 360 - |\theta_p - \theta_g|),$$

694 which correctly accounts for circular periodicity (e.g., $0^\circ \equiv 360^\circ$). The completion score is defined
 695 as:

$$696 \text{CD} = 1 - \frac{\Delta\theta}{\theta_{\max}},$$

697

698 where θ_{\max} is the maximum possible deviation (180°). A CD of 1 means the rotation is perfectly
 699 aligned, 0.5 means a misalignment of 90° , and 0 means an opposite alignment (180° difference).

700 **Explanation.** This metric gives proportionate credit for predictions that are close to the correct
 701 angle, which more accurately reflects an agent’s capability in near-solved cases compared to a binary
 702 pass/fail judgment.

C DETAILED VISIT PROBABILITY OF WEBSITES

702

703

704

705

706

707

708

709

710

711

712

713

714

715

716

717

718

719

720

721

722

723

724

725

726

727

728

729

730

731

732

733

734

735

736

737

738

739

740

741

742

743

744

745

746

747

748

749

750

751

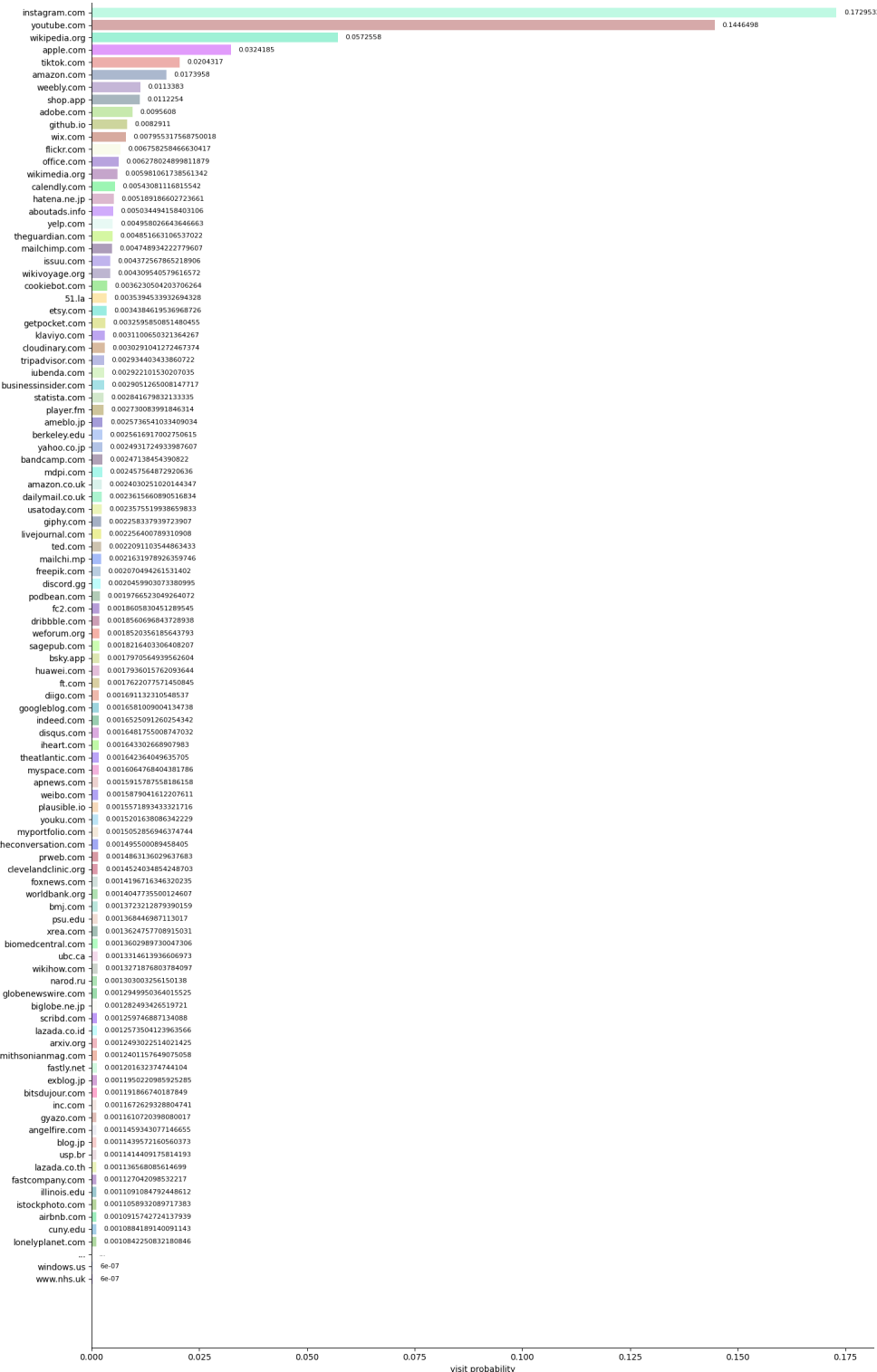
752

753

754

755

Figure 8: Detailed visit frequencies distribution of the 2,095 websites with deployed CAPTCHAs. The top 10 websites account for nearly half of the total traffic, reflecting real-world internet patterns.

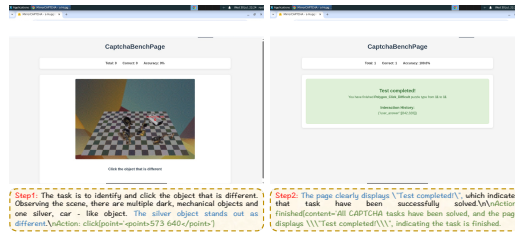


756 D ADDITIONAL REASONING PROCESS ON MIRRORCAPTCHA
757

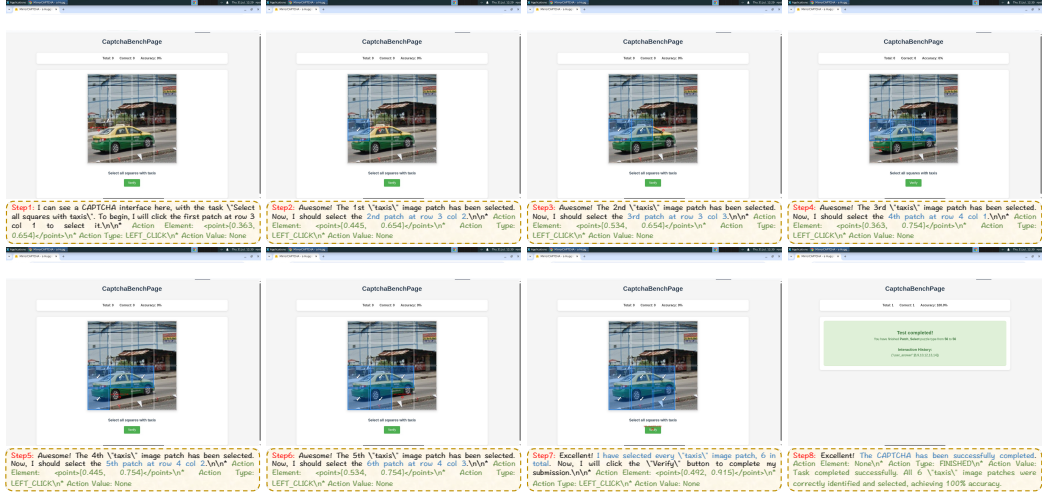
758 We provide further examples of CAPTCHA-solving processes to illustrate how the web agent interacts
759 with real-world webpages. These cases highlight the agent's ability to interpret and reason over
760 CAPTCHA puzzles, make decisions, and execute corresponding interactive actions.



770 Figure 9: CAPTCHA puzzle: Find and select the unpaired shape in the image.



778 Figure 10: CAPTCHA puzzle: Click the object that is different.



799 Figure 11: CAPTCHA puzzle: Select all squares with taxis.

810
811
812
813
814
815
816
817
818
819



Figure 12: CAPTCHA puzzle: Pick one square showing two identical objects, then click submit.

820
821
822
823
824
825
826
827
828
829
830
831
832
833

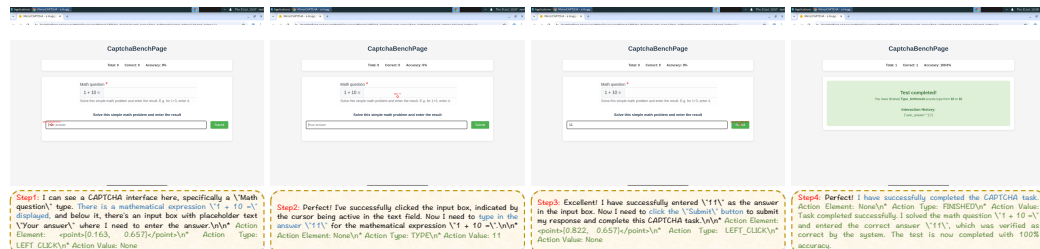


Figure 13: CAPTCHA puzzle: Solve the math problem and enter the result.

834
835
836
837
838
839
840
841
842
843
844
845
846
847

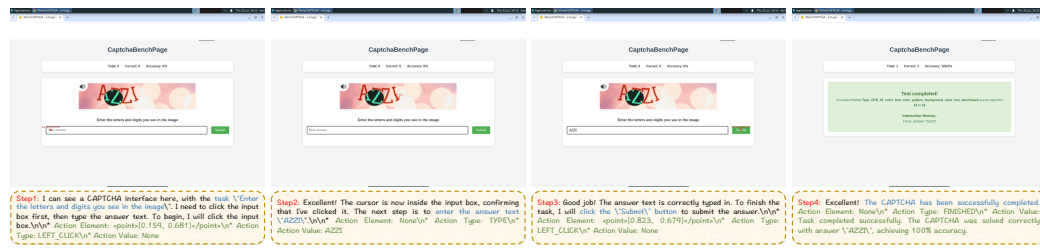


Figure 14: CAPTCHA puzzle: Enter the letters and digits shown in the image.

848
849
850
851
852
853
854
855
856
857
858
859
860
861
862
863

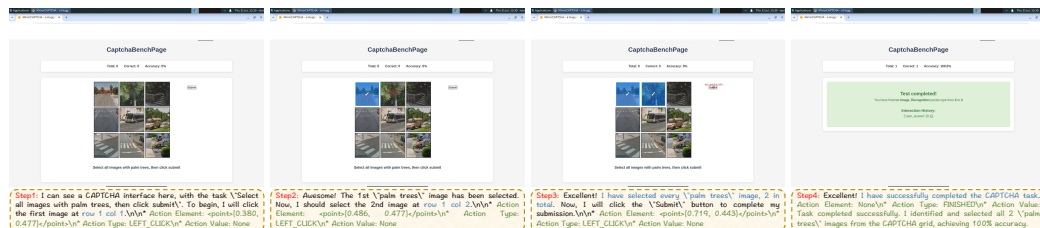


Figure 15: CAPTCHA puzzle: Select all images with palm trees, then click submit.

864
865
866
867
868
869
870
871
872
873
874
875
876
877
878
879
880
881
882

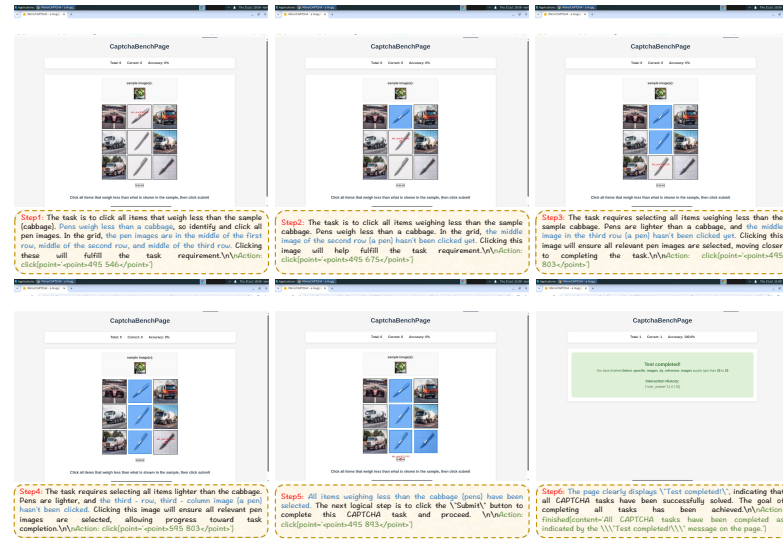


Figure 16: CAPTCHA puzzle: Click all items that weigh less than the sample.

883
884
885
886
887
888
889
890
891
892
893
894
895

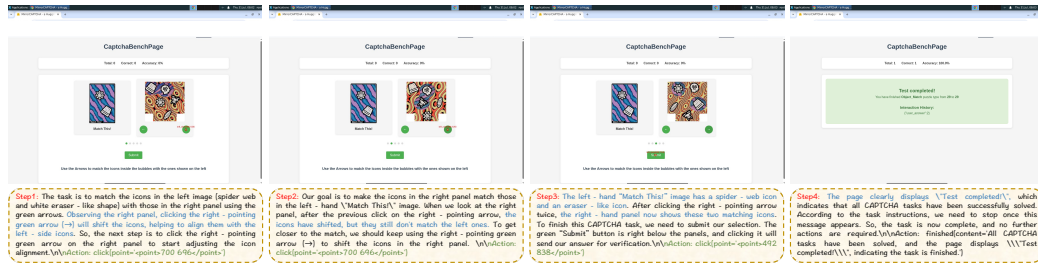


Figure 17: CAPTCHA puzzle: Use Arrows to match the icons inside the bubbles with those on the left.

896
897
898
899
900
901
902
903
904
905
906
907
908
909
910
911
912
913
914
915
916
917

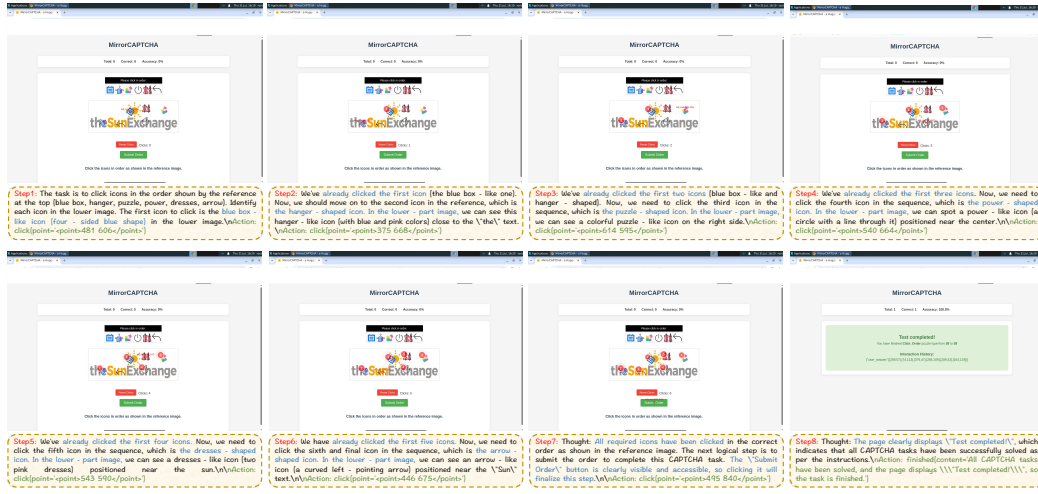


Figure 18: CAPTCHA puzzle: Click the icons in order shown in the reference images.